Int. J. Heat Mass Transfer. Vol. 34, No. 3, pp. 819–833, 1991
Printed in Great Britain

0017–9310/91 $3.00+0.00


# Forced convection heat transfer in microencapsulated phase change material slurries: flow in circular ducts

P. CHARUNYAKORN,† S. SENGUPTA‡ and S. K. ROY
Department of Mechanical Engineering, University of Miami, Coral Gables, FL 33124, U.S.A.

(*Received* 29 *August* 1989 *and in final form* 8 *May* 1990)

**Abstract**—The heat transfer characteristics of microencapsulated phase change material slurry flow in circular ducts are presented in this paper. The energy equation is formulated by taking into consideration both the heat absorption (or release) due to the phase change process and the conductivity enhancement induced by the motion of the particles. The heat source or heat generation function in the energy equation is derived from solutions for freezing or melting in a sphere. The correlation for the effective conductivity of the slurry is obtained based on available analytical and experimental results. The governing parameters are found to be the particle concentration, a bulk Stefan number, the duct/particle radius ratio, the particle/fluid conductivity ratio, and a modified Peclet number. For low temperature applications, it is found that the dominant parameters are the bulk Stefan number and concentration. The numerical solutions show that heat fluxes about 2–4 times higher than single phase flow may be achieved by a slurry system.

## INTRODUCTION

MAJOR factors that make phase change materials very attractive for thermal energy storage and thermal control are high energy storage density and small temperature variation. As a result, a wide variety of applications have been suggested and implemented in practice [1]. Recently, a new technique of utilizing phase change materials in energy storage and thermal control systems has been investigated [2–6]. In this approach, the phase change material is microencapsulated and suspended in a heat transfer fluid to form a phase change slurry.

The concept of a phase change slurry has been made possible by advances in microencapsulation technology over the past decade. Since the ratio of surface area to volume of small particles is relatively large, the heat transfer rate per unit volume to or from the material in the particles is high. The slurry also serves as both the energy storage and heat transfer media, and the requirement of separate heat transfer media is therefore eliminated [7]. In addition, encapsulating the phase change material in small capsules is expected to eliminate any segregation during phase change [8]. A phase change slurry also benefits from heat transfer enhancement found in the flow of suspensions as reported by several investigators [9–14].

While all the preliminary studies and experiments indicate promising applications of the phase change slurry as a heat transfer and storage medium, data necessary for design is very incomplete. The lack of a general, systematic approach in earlier studies makes it difficult to interpret or evaluate many of the results. Furthermore, most studies have concentrated on the materials and thermal storage aspects of phase change slurries. As a result, the most important aspect of such slurries, namely their heat transfer enhancing capability, has received only limited attention [3, 9–10, 14]. In order to address this problem, a theoretical model describing the forced convection heat transfer with a phase change material slurry in a circular duct flow has been developed in this paper. Based on this model, numerical solutions valid for low temperature applications have been obtained.

## FORMULATION OF THE PROBLEM

Figure 1(a) shows a schematic diagram describing the problem. The flow field in the duct may be divided into two regions, a melting (or freezing) region and a fully melted (or frozen) region. These two regions are separated from each other by a phase change 'interface' which is a locus of points at which the particles become completely melted (or frozen). The melting (or freezing) region with the particles at different stages of the phase change process occupies the central portion of the flow field. The fully melted (or frozen) region is bounded by the tube wall and the 'interface'. The phase change material in the capsules in this region is either solely liquid or solely solid since the phase change process has been completed. The following assumptions are made in formulating the governing equations:

(1) The maximum microcapsule concentration considered in this study is limited to 0.25. The fluid can therefore be considered as Newtonian [15–17]. Cases with higher concentrations, where non-Newtonian effects are important, have not been con-

†Current address: Faculty of Engineering, Chulalongkorn University, Thailand.
‡Current address: School of Engineering, University of Michigan, Dearborn, Michigan, U.S.A.

## NOMENCLATURE

| | |
|---|---|
| $B$ | constant, equation (9) |
| $Bi$ | Biot number |
| $C$ | specific heat |
| $c$ | volumetric concentration of suspended particles |
| $d$ | particle diameter |
| $D$ | duct diameter |
| $e$ | velocity gradient |
| $f$ | conductivity enhancement function, equation (9) |
| $h$ | heat transfer coefficient |
| $i$ | mesh point index in the radial direction |
| $I$ | value of index $i$ on the wall |
| $k$ | thermal conductivity |
| $L$ | latent heat of phase change material; duct length |
| $m$ | constant, equation (9) |
| $Nu$ | Nusselt number |
| $n$ | mesh point index in the axial direction |
| $Pe$ | Peclet number |
| $Pr$ | Prandtl number |
| $q$ | heat flux |
| $\dot{Q}$ | heat transfer rate |
| $R$ | radius |
| $Re$ | Reynolds number |
| $r$ | duct radial coordinate; $r_p$ is the interface location in a particle |
| $S$ | heat source or sink |
| $Ste$ | Stefan number |
| $T$ | temperature |
| $\Delta T_{ln}$ | log mean temperature difference |
| $t$ | time |
| $u$ | velocity in the $X$-direction |
| $V$ | volume |
| $x$ | coordinate in the axial direction |
| $z$ | 'interface' location, measured from the wall. |

Greek symbols

| | |
|---|---|
| $\alpha$ | thermal diffusivity |
| $\beta$ | reciprocal of $Bi$ |
| $\theta$ | temperature |
| $\mu$ | dynamic viscosity |
| $\nu$ | kinematic viscosity |
| $\rho$ | density. |

Subscripts

| | |
|---|---|
| 1 | dimensionless variables |
| b | bulk fluid (slurry) |
| bm | bulk mean values |
| d | duct |
| e | effective |
| f | suspending fluid; final-stage melting |
| m | melting point |
| p | particles |
| s | solid-phase portion in a particle |
| w | wall |
| $x$ | at axial position $x$. |

Superscript

| | |
|---|---|
| · | rate of change with respect to time. |

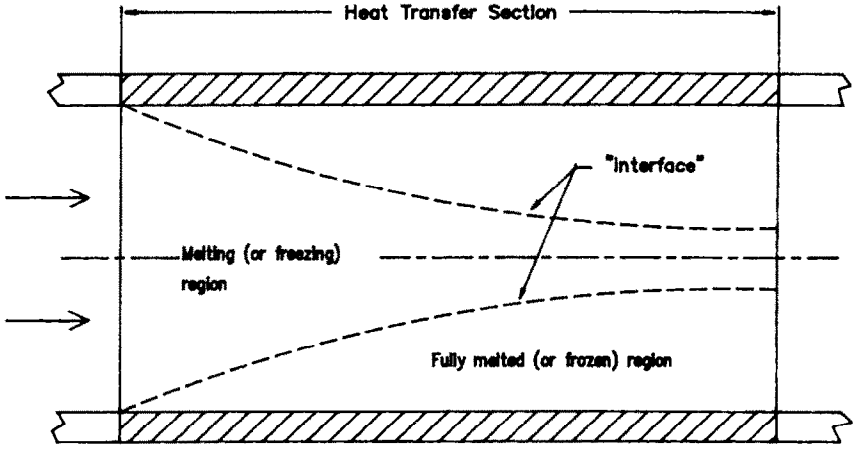


FIG. 1(a). Heat transfer of phase change slurry in a duct.

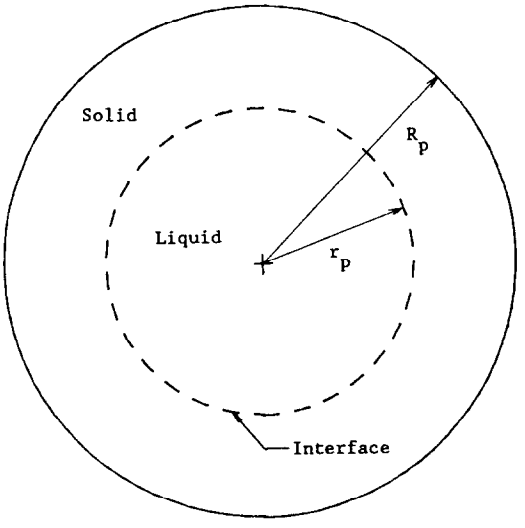


FIG. 1(b). Freezing in a sphere.

sidered, since neither the viscosity, nor the thermal conductivity, can be correlated with the particle concentration and related parameters.

(2) The flow is assumed to be incompressible and laminar. It is also hydrodynamically fully developed and uniform at the melting/freezing temperature of the phase change particles when it enters the heat transfer section. The model developed in this paper can also be used in case the suspension is subcooled as it enters the duct, but the analysis has been limited to the zero subcooling case in order to reduce the number of parameters.

(3) The particles are rigid inert spheres with density approximately equal to that of the suspending fluid. Though this condition may not be achieved under all conditions, stratification and sedimentation can be minimized by using microcapsules of very small diameters.

(4) The slurry is assumed to be homogeneous and therefore has constant bulk properties, except for the thermal conductivity which is a function of the local shear [11–13] and varies across the flow field. This assumption is valid when the particle-to-duct diameter ratio is small [18, 19]. For low particle-to-duct diameter ratios, radial migration effects are also negligible [20, 21]. For suspensions of very small particles (0.1–20 $\mu$m) which are often flocculated, the degree of uniformity may be increased by adding a suitable dispersing agent [22].

(5) The wall effect, which creates a particle-free layer next to the wall, is assumed to be negligible. This is valid for a small particle/duct diameter ratio since the particle-free layer is approximately 0.5–1 particle diameter [21, 23].

(6) The coating of the particles is very thin, and the particles therefore consist entirely of the phase change material. This is not actually achieved in practice where the encapsulating material may be 10–20% of the total microcapsule volume. However, in most cases, errors can be expected to be quite small as long as the concentration is defined based on the actual volume of the phase change material. Any further corrections in the bulk properties due to the encapsulating material should be negligible since its mass fraction in the slurry is only of the order of 5%.

Based on the above assumptions the governing equations are:

*Velocity profile*

$$u = 2u_m\left[1-\left(\frac{r}{R}\right)^2\right]. \tag{1}$$

*Energy equation*

$$\rho Cu\frac{\partial T}{\partial x} = \frac{\partial}{\partial r}\left(k\frac{\partial T}{\partial r}\right)+\left(\frac{k}{r}\frac{\partial T}{\partial r}\right) + \frac{\partial}{\partial x}\left(k\frac{\partial T}{\partial x}\right)+\mu\left(\frac{\partial u}{\partial r}\right)^2+S \tag{2}$$

with the following boundary conditions:

$T = T_w$ at $r = R_d$,

for constant wall temperature (3a)

$$\frac{\partial T}{\partial r} = -\frac{q_w}{k_{e,w}} \quad \text{at } r = R_d,\ x > 0,$$

for constant wall heat flux (3b)

$$\frac{\partial T}{\partial r} = 0 \quad \text{at } r = 0,\ x > 0 \tag{3c}$$

$$T = T_m \quad \text{at } x = 0,\ r < R_d \tag{3d}$$

$$r_p = R_p \quad \text{at } x = 0. \tag{3e}$$

The density and specific heat in this equation are those of the slurry, and are evaluated by the weighted mean method. The thermal conductivity is an effective value which includes microconvection due to the eddy motion of fluid around the particles. The heat source function $S$ is the result of the change of phase in the suspended particles. These are discussed in greater detail below.

*Thermal conductivity*

The thermal conductivity of static dilute suspensions, $k_b$, can be evaluated from Maxwell's relation [24]

$$\frac{k_b}{k_f} = \frac{2+k_p/k_f+2c(k_p/k_f-1)}{2+k_p/k_f-c(k_p/k_f-1)}. \tag{4}$$

Because of the enhancement created by the particle/fluid interactions, the effective conductivity of flow slurries is higher than that predicted by equation (4). Leal [25] studied conductivity enhancement in dilute suspensions at very low particle Peclet numbers and obtained the following relation, for suspensions with equal particle and fluid conductivity:

$$\frac{k_e}{k_f} = 1 + 3.0c\, Pe_p^{1.5} \tag{5}$$

where $Pe_p$ is the particle Peclet number

$$Pe_p = \frac{ed^2}{\alpha_f}. \tag{6}$$

Nir and Acrivos [26] applied a similar model to dilute suspension flow at very high particle Peclet numbers and obtained a relation

$$\frac{k_e}{k_f} = 1 + Ac\, Pe_p^{1/11} \tag{7}$$

where $A$ is a constant the value of which may be determined experimentally. Sohn and Chen [13] conducted experiments at moderate Peclet numbers and proposed a correlation of the form

$$\frac{k_e}{k_b} = F(c, \ldots) Pe_p^m \tag{8}$$

where $F$ is an undetermined function. Based on the results discussed above, a general correlation of the form

$$\frac{k_e}{k_b} = f = 1 + Bc\, Pe_p^m \tag{9}$$

is used in this study. Constants $B$ and $m$, the values of which depend on the particle Peclet numbers, have been evaluated as follows. At low Peclet numbers, the values are those given in equation (5), i.e. $B = 3.0$ and $m = 1.5$. At high Peclet number, the value of $m$ is obtained from equation (7), i.e. $m = 1/11$. The experimental results from ref. [13] are then used to evaluate $B$ and $m$ at moderate Peclet numbers, which come out as 1.8 and 0.18, respectively. In order to reduce the wall effects, only the data of the polystyrene suspensions with larger channel gap to particle diameter ratio were used to obtain the above values. From the intersection between the curves of low and moderate Peclet numbers, the low-to-moderate transition Peclet number was found to be approximately 0.67. For higher particle Peclet numbers, Sohn and Chen's [13] data seem to show a transition at a Peclet number of about 250. Using this transition value, $B$ for the high Peclet number region was found to be 3.0. The final correlation for the entire range is shown graphically in Fig. 2.

An alternative approach to obtain the effective thermal conductivity would be to use a power-law model for the thermal conductivity as done by Sohn and Chen [14]. The above correlation is then a special form of the general power law model. Since the problem of effective thermal conductivity of suspensions is still essentially unresolved, such an approach would seem to be more appropriate. Nevertheless, the use of an explicit relation as above has the advantage of reducing the number of parameters related to the problem. In addition, the actual errors caused by the use of the above thermal conductivity relation is quite small even in the absence of phase change as shown in a later section. Once phase change is taken into account, any effects are marginal, since results show that the effect of particles on the Nusselt number is very small as compared to those related to the phase change phenomenon.

*Heat source S*

The source $S$ represents heat released or absorbed by the phase change process in the particles. It is obtained from the product of the heat generation or absorption rate per particle and the number of particles per unit volume of the slurry. Since the local Stefan number of the phase change process involving small spheres is generally low, the heat transfer rate per particle is evaluated as follows:

$$\dot{Q}_p = \rho_p \dot{V}_s L = 4\pi k_p (T_m - T) \frac{r_p}{1 - (1-\beta_p) r_{p1}} \tag{10a}$$

where $\dot{V}_s$ is the rate of change of the volume of the solid phase in the sphere

$$\dot{V}_s = -4\pi r_p^2 \, dr_p/dt \tag{10b}$$

and the interface location in the microcapsule, $r_p$ (Fig. 1(b)), is given by Tao's [27] solution

$$t_1 = (1 - r_{p1}^2)/2 + (1 - r_{p1}^3)(\beta_p - 1)/3 \tag{10c}$$

where $R_p$ is the particle radius, $t_1$ the non-dimensional time given by $t(\alpha_p/(R_p^2))(C_p(T_m - T)/L)$, and $\beta_p = k_p/h_p R_p = 1/Bi_p$. The heat source term therefore becomes

$$S = \dot{Q}_p N = 3ck_p \frac{(T_m - T)}{R_p^2} \frac{r_{p1}}{1 - (1-\beta) r_{p1}} \tag{11}$$

where $N$ is the number of microcapsules per unit volume.

The heat transfer coefficient around spheres can be evaluated from the conduction model based on the effective thermal conductivity which includes the effects of molecular diffusion and eddy convection around the particles. This leads to

$$Bi_p = \frac{k_e}{k_p} \frac{2(1-c)}{(2 - 3c^{1/3} + c)}. \tag{12}$$

The stage of freezing of an individual particle, i.e. the value of $r_{p1}$, can be determined from a heat balance equation given below. The left-hand side represents the energy released by the phase change process in a particle, and the right-hand side is the cumulative heat transfer between that particle and the surrounding fluid

$$\tfrac{4}{3}\pi (R_p^3 - r_p^3) L \rho_p = \int_0^t \dot{Q}_p \, dt = \int_0^x \dot{Q}_p \frac{dx}{u}$$

which can be rearranged as

$$r_p = \left[ R_p^3 - R_p \frac{3k_p}{L\rho_p} \int_0^x (T_m - T) \frac{r_p}{1 - (1-\beta) r_{p1}} \frac{dx}{u} \right]^{1/3}. \tag{13}$$

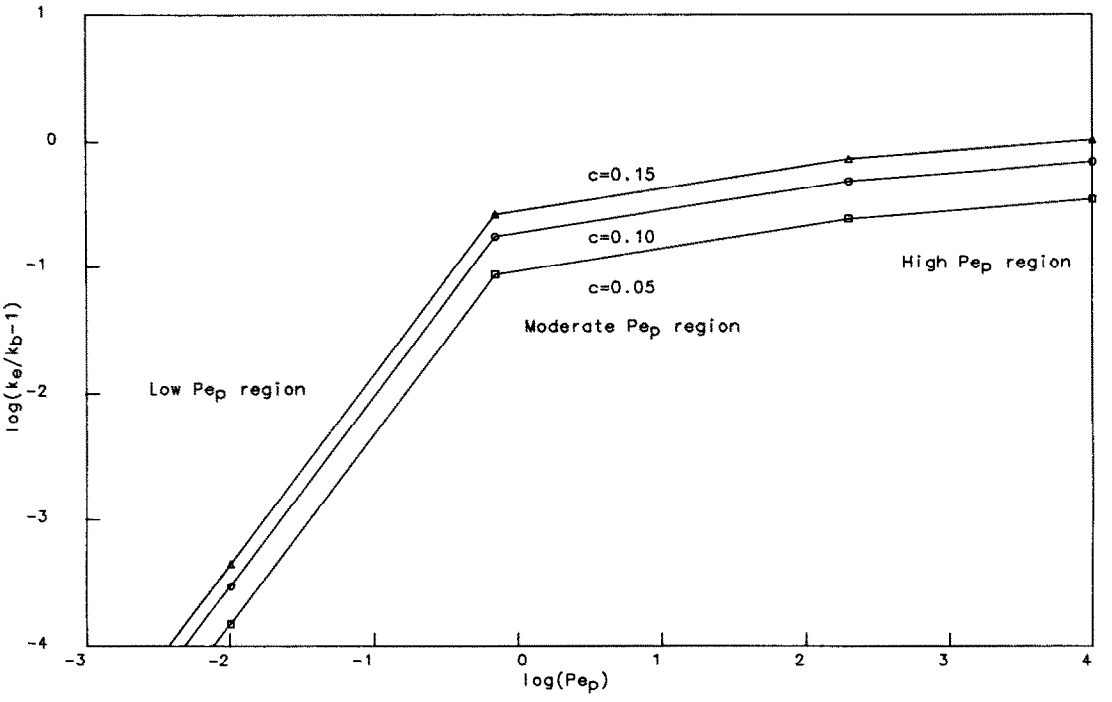


FIG. 2. Thermal conductivity enhancement as a function of particle Peclet number and particle concentration.

It must be noted that the above equations are valid for both the melting and the freezing case since Tao's [27] solution, which was obtained for freezing in a sphere, is also valid for melting if natural convection effects are neglected. Previous studies have already shown that natural convection is negligible for very small spheres [29, 30].

## METHOD OF SOLUTION

*Nondimensionalization*

The governing equations developed are first non-dimensionalized using the following dimensionless variables:

$$r_1 = \frac{r}{R_d}, \quad x_1 = \frac{x}{R_d (Re\,Pr)_b}; \quad u_1 = \frac{u}{u_m} \tag{14}$$

$$\theta = \frac{(T - T_w)}{(T_m - T_w)}, \quad \text{for constant wall temperature} \tag{15a}$$

$$\theta = \frac{(T_m - T)}{(q_w R_d / k_b)}, \quad \text{for constant wall heat flux.} \tag{15b}$$

The non-dimensional velocity profile retains an identical form as equation (1), and the energy equation becomes

$$\frac{u_1}{2}\frac{\partial \theta}{\partial x_1} = f\frac{\partial^2 \theta}{\partial r_1^2} + \left(\frac{f}{r_1} + \frac{\partial f}{\partial r_1}\right)\frac{\partial \theta}{\partial r_1} + \frac{f}{Pe_b^2}\frac{\partial^2 T}{\partial x_1^2} - 2Br'\left(\frac{\partial u_1}{\partial r_1}\right)^2 + S_1(r_1, x_1, \theta) \tag{16}$$

where

$$f = 1 + Bc8^m \{Pe_f (R_p/R_d)^2\}^m r_1^m \tag{17a}$$

$$\frac{\partial f}{\partial r_1} = Bcm8^m \{Pe_f (R_p/R_d)^2\}^m r_1^{m-1} \tag{17b}$$

$$Pe_f = \frac{2R_d u_m}{\alpha_f} \tag{17c}$$

$$Pe_b = \frac{2R_d u_m}{\alpha_b}. \tag{17d}$$

For constant wall temperature

$$Br' = \text{Brinkmann number} = \frac{\mu u_m^2}{2k_b (T_w - T_m)} \tag{18}$$

$$S_1 = 3c(1-\theta)\frac{k_p R_d^2}{k_b R_p^2}\frac{r_{p1}}{1-(1-\beta)r_{p1}} \tag{19}$$

$$r_{p1} = \left[1 - 6c\,Ste_{b,T}\frac{k_p R_d^2}{k_b R_p^2}\int_0^{x_1}\frac{r_{p1}}{1-(1-\beta)r_{p1}}(1-\theta)\frac{dx_1}{u_1}\right]^{1/3} \tag{20a}$$

where

$$Ste_{b,T} = \text{bulk 'Stefan number'} = \frac{C_b |T_w - T_m|}{cL(\rho_p/\rho_b)} = \frac{\text{sensible heat of slurry}}{\text{'latent heat' of slurry}} \tag{20b}$$

For the constant wall heat flux

$$Br = \frac{\mu u_m^2}{2R_d q_w} \tag{21}$$

$$S_1 = -3c\frac{k_p R_d}{k_b R_p^2}\frac{r_{p1}}{1-(1-\beta_p)r_{p1}}\theta \tag{22}$$

$$r_{p1} = \left[1-6c\,Ste_{b,H}\frac{k_p R_d^2}{k_b R_p^2}\int_0^{x_1}\frac{r_{p1}}{1-(1-\beta_p)r_{p1}}\theta\frac{dx_1}{u_1}\right]^{1/3} \tag{23}$$

where

$$Ste_{b,H} = \frac{C_b|q_w R_d/k_b|}{cL(\rho_p/\rho_b)}. \tag{24}$$

In the present problem, only the case where axial conduction is negligible, i.e. when the bulk Peclet number, $Pe_b$, is greater than 100 [28], is considered. For small Brinkmann numbers, the viscous dissipation can be neglected, and the energy equation reduces to

$$\frac{u_1}{2}\frac{\partial\theta}{\partial x} = f\frac{\partial^2\theta}{\partial r_1^2} + \left(\frac{f}{r_1}+\frac{\partial f}{\partial r_1}\right)\frac{\partial\theta}{\partial r_1} + S_1(x_1, r_1, \theta). \tag{25a}$$

The boundary conditions, (3a)–(3e), become

$$\theta = 1 \quad \text{at } r_1 = 1,\ x_1 > 0, \quad \text{for constant wall temperature} \tag{25b}$$

$$\frac{\partial\theta}{\partial r_1} = \frac{1}{f_w} \quad \text{at } r_1 = 1,\ x_1 > 0, \quad \text{for constant wall heat flux} \tag{25c}$$

$$\frac{\partial\theta}{\partial r_1} = 0 \quad \text{at } r_1 = 0,\ x_1 > 0 \tag{25d}$$

$$\theta = 1 \quad \text{at } x_1 = 0,\ r_1 < 1, \quad \text{for constant wall temperature} \tag{25e}$$

$$\theta = 1 \quad \text{at } x_1 = 0,\ r_1 < 1, \quad \text{for constant wall heat flux} \tag{25f}$$

$$r_{p1} = 1 \quad \text{at } x_1 = 0. \tag{25g}$$

*Discretization of governing equations*

An analytical solution for the governing equations cannot be obtained because of the complexity of the source term. A numerical solution using an implicit finite difference method was therefore used. The energy equation (equation (25a)) can be written in a difference form as

$$-\left(2\frac{f_i d}{u_{1,i}} - \frac{f_i d}{iu_{1,i}} - \frac{d}{u_{1,i}}\frac{\partial f}{\partial r_1}\Delta r_1\right)\theta_{i-1}^{n+1} + \left(1+4\frac{f_i d}{u_{1,i}}\right)\theta_i^{n+1} - \left(2\frac{f_i d}{u_{1,i}} + \frac{f_i d}{iu_{1,i}} + \frac{d}{u_{1,i}}\frac{\partial f}{\partial r_1}\Delta r_1\right)\theta_{i+1}^{n+1} = \theta_i^n + 2S_{1,i}^{n+1}\frac{\Delta x_1}{u_{1,i}} \tag{26}$$

where $d = \Delta x_1/(\Delta r_1)^2$, $n$ is the mesh point index in the $x_1$-direction, $i$ the mesh point index in the $r_1$-direction $= 0, 1, 2, \ldots, I$.

Equations (25a) and (26) are applicable for every mesh point except the ones along the centerline. Inspection of energy equation (25a) reveals that the terms involving the division of $\partial\theta/\partial r_1$ by $r_1$ on the right-hand side of the equation are indeterminate of the form 0/0 at the center. By applying L'Hospital's rule to $(\partial\theta/\partial r_1)/r_1$ as $r_1$ approaches zero, the differential and difference energy equations reduce to

$$\frac{u_1}{2}\frac{\partial\theta}{\partial x_1} = 2f\frac{\partial^2\theta}{\partial r_1^2} + \frac{\partial f}{\partial r_1}\frac{\partial\theta}{\partial r_1} + S_1(r_1, x_1, \theta) \tag{27a}$$

$$\left(1+8\frac{f_0 d}{u_{1,0}}\right)\theta_0^{n+1} - 8\frac{f_0 d}{u_{1,0}}\theta_1^{n+1} = \theta_0^n + 2S_{1,0}^{n+1}\frac{\Delta x_1}{u_{1,0}} \tag{27b}$$

where the boundary condition $\theta_{-1} = \theta_1$ and $(\partial f/\partial r_1) = 0$ due to symmetry have been used. The heat source, equations (18) and (22), is expressed in the form

$$S_{1,i}^{n+1} = C_{s1,i}^{n+1}(1-\theta_i^{n+1}), \quad \text{for constant wall temperature} \tag{28a}$$

$$S_{1,i}^{n+1} = -C_{s1,i}^{n+1}\theta_i^{n+1}, \quad \text{for constant wall heat flux} \tag{28b}$$

where

$$C_{s1,i} = 3c\frac{k_p R_d^2}{k_b R_p^2}\frac{r_{p1}}{1-(1-\beta_p)r_{p1}}. \tag{29}$$

Equations (28) and (29) are applicable to any marching step in $x_1$ during which the particles have not completely melted or frozen. For the marching step during which complete phase change takes place, the source term becomes

$$S_{f,i} = \frac{r_{p1,i}^3}{2Ste_b}\frac{u_{1,i}}{\Delta x_1}, \quad \text{for constant wall temperature} \tag{30a}$$

$$S_{f,i} = -\frac{r_{p1,i}^3}{2Ste_b}\frac{u_{1,i}}{\Delta x_1}, \quad \text{for constant wall heat flux.} \tag{30b}$$

Finally, in the fully melted region, $S_{f,i} = 0$.

The system of different equations are now solved simultaneously at each marching step. Since the coefficient matrix of the system is tridiagonal, it can be solved by using the Thomas algorithm. However, since the coefficient $C_{s1,i}$ is a function of $r_{p1}$ which is an implicit function of temperature, it is solved in an iterative fashion.

*Verification of model and code*

Table 1 summarizes the comparison between analytical solutions and the present numerical solutions

Table 1. Comparison of analytical and numerical mean Nusselt numbers

| | Analytical solutions[a] | | Present work | | | |
|---|---|---|---|---|---|---|
| $x_1$ | $\theta_{bm}$ | $Nu_m$ | $\theta_{bm}$ | $Nu_m$[b] | $Nu_m$[c] | $Nu_m$[d] |
| 0.001 | 0.9618 | 19.50 | 0.9620 | 22.06 | 20.65 | 19.37 |
| 0.01 | 0.8362 | 8.943 | 0.8364 | 9.254 | 9.180 | 8.932 |
| 0.04 | 0.6280 | 5.815 | 0.6282 | 5.906 | 5.926 | 5.811 |
| 0.10 | 0.3953 | 4.641 | 0.3954 | 4.685 | 4.718 | 4.639 |
| 0.20 | 0.1897 | 4.156 | 0.1898 | 4.184 | 4.220 | 4.154 |
| 0.40 | 0.04393 | 3.906 | 0.04401 | 3.929 | 3.965 | 3.904 |

[a] From ref. [34].
[b] From equation (32), wall temperature gradient evaluated from second-degree polynomial.
[c] From equation (32), wall temperature gradient evaluated from first-degree polynomial.
[d] From equation (34).

for pure fluid flow. The mean Nusselt number in the last column in Table 1 is calculated from [28]

$$Nu_m = \frac{1}{2x_1} \ln \frac{1}{\theta_{bm}} \tag{31}$$

which is applicable to single phase flow without a heat source only. The numerical Nusselt number based on a first degree polynomial appears to be more accurate at small $x_1$ but less accurate at large $x_1$ compared to a second degree polynomial. All the Nusselt numbers for slurry flow with phase change were obtained based on a first degree polynomial approximation.

Figures 3–5 show the comparison between the mean Nusselt numbers obtained from the present numerical method for a slurry flow without phase change and the experimental results [11]. The relatively higher experimental values may be caused in part by the viscosity variation since the difference between the wall and average fluid temperature was relatively large. To account for such effects, the correction factor, $(\mu_b/\mu_w)^{0.14}$, from ref. [31] was initially used. Introduction of the correction factor to the numerical results brings the mean Nusselt numbers in Fig. 3 to within 6% for $c = 0.046$ and within 12% for $c = 0.088$, and brings the results in Fig. 4 to within 9%. Unfortunately however, this adjustment creates even larger discrepancies for results in Fig. 5, and further explanation is obviously required.

Two features of the experimental results suggest a possible explanation. First, the flow shown in Fig. 5 is well into the thermally fully developed region while those in Figs. 3 and 4 are still in the developing stage. Secondly, the influence of concentration appears to be substantially weakened for the results in Fig. 5. These observations suggest that the radial migration effects may be significant since the particle/duct diameter ratio is not sufficiently small. The effects are more appreciable when the slurry flows further downstream and the particles more further away from the wall. The extent of the effects cannot be evaluated

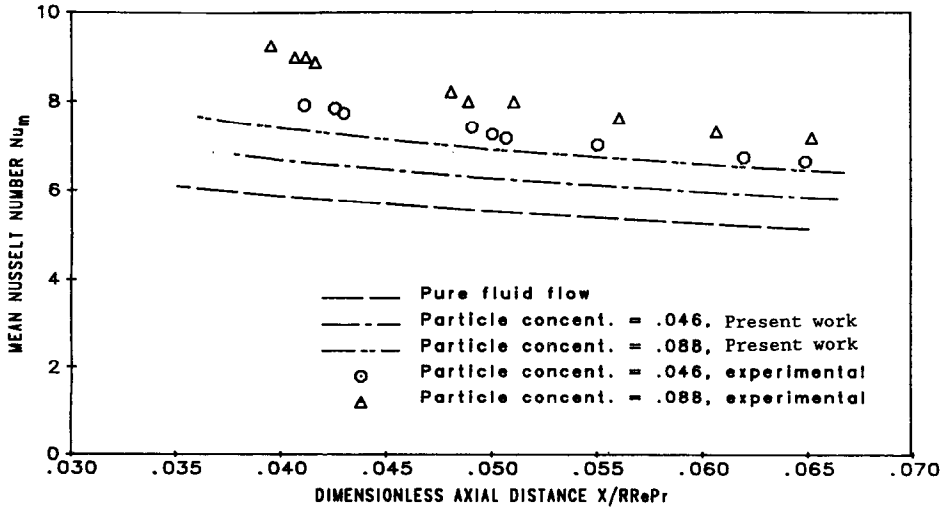


FIG. 3. Comparison of numerical results and experimental results of Ahuja [11] for heat transfer in a circular duct. Suspension: 100 $\mu$m polystyrene spheres in 5.2% aqueous NaCl solution. Duct diameter = 0.002 m. Duct length = 0.4 m. Constant wall temperature.

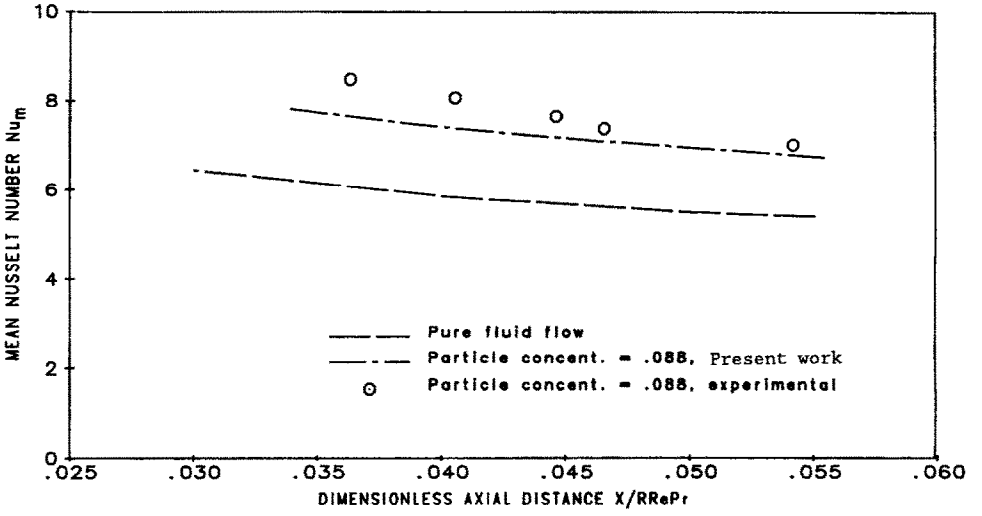


FIG. 4. Comparison between numerical results and experimental results of Ahuja [11] for heat transfer in a circular duct. Suspension: 100 $\mu$m polystyrene spheres in 20% wt. aqueous glycerine solution. Duct diameter = 0.002 m. Duct length = 0.4 m. Constant wall temperature.

quantitatively because the Reynolds numbers are outside the range of the model developed in ref. [20]. Further investigation is needed in this area.

Another possible reason for the discrepancy lies in the definition of a 'dilute' suspension. The theoretical models used in deriving the above correlation consider a dilute suspension where effects of particle-to-particle collisions are neglected. Since the concentration limit for dilute suspensions is uncertain, it is quite possible that the errors are due to the assumption that the suspensions studied in ref. [11] were dilute.

In order to verify numerical convergence of the solution, a number of test runs have been performed for different grid sizes. For the constant wall temperature boundary condition, it was found that the solutions converged for $r_1$ and $x_1$ step sizes of 0.025 and 0.00005, respectively. On the other hand, the solution for the constant wall heat flux boundary condition required much finer grids with $r_1$ and $x_1$ of 0.00625 and 0.00005, respectively. These were the final grid sizes used to obtain the results for the two cases.

## RESULTS AND DISCUSSION

The parameters for the present problem are the volumetric particle concentration, the bulk 'Stefan

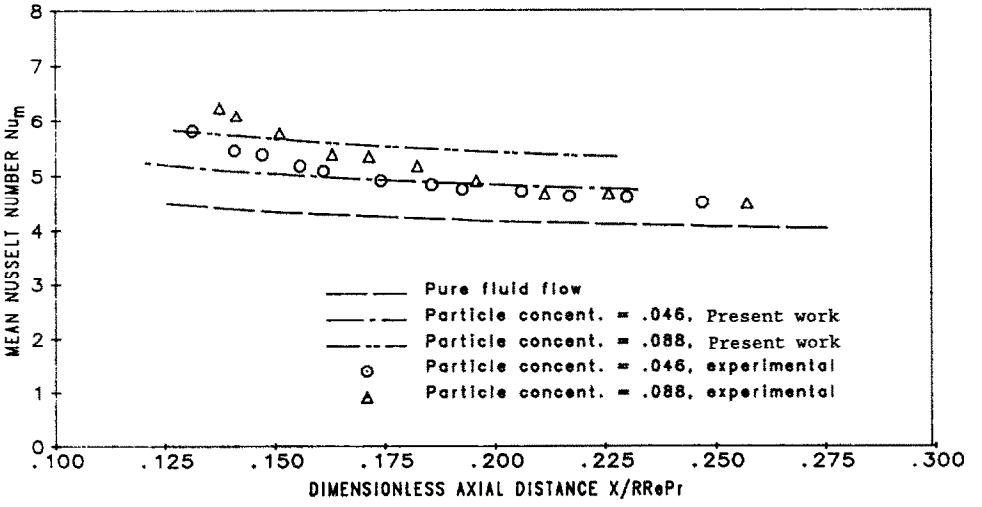


FIG. 5. Comparison between numerical results and experimental results of Ahuja [11] for heat transfer of suspension in a circular duct. Suspension: 50 $\mu$m polystyrene spheres in 5.2% aqueous NaCl solution. Duct diameter = 0.001 m. Duct length = 0.55 m. Constant wall temperature.

number', the duct/particle radius ratio, the particle/fluid thermal conductivity ratio, and a modified Peclet number $Pe_f(R_p/R_d)^2$. The effects of these parameters were studied in the ranges of parameter values typical for low temperature applications (< 100°C): $0.1 \leqslant c \leqslant 0.25$, $50 \leqslant R_d/R_p \leqslant 400$, $0.25 \leqslant Pe_f(R_p/R_d)^2 \leqslant 4.0$, $0.25 \leqslant k_p/k_f \leqslant 4.0$, and $0.25 \leqslant Ste_b \leqslant 2.0$ for the constant temperature case and $1.0 \leqslant Ste_b \leqslant 5.0$ for the constant heat flux case.

The solutions are presented in terms of mean Nusselt number (for constant wall temperature), local Nusselt number (for constant wall heat flux), bulk mean temperature, and 'interface' location. These four sets of information are necessary for thermal design as demonstrated by the sample calculations in the Appendix. The mean Nusselt number is defined as

$$Nu_m = \frac{2h_m R_d}{k_b} = \frac{2R_d q_w}{k_b \Delta T_{ln}} = 4f_w \frac{\ln \theta_{bm}}{\theta_{bm} - 1} \frac{1}{x_1} \int_0^{x_1} \left( -\frac{\partial \theta}{\partial r_1} \right)_w dx_1' \quad (32)$$

where $q_w$ is the mean wall heat flux and $\Delta T_{ln}$ the log mean temperature difference. The local Nusselt number is defined as

$$Nu_x = \frac{2R_d h_x}{k_b} = \frac{2}{\theta_w - \theta_{bm}}. \quad (33)$$

The graphs of 'interface' location, which are expressed in terms of dimensionless distance $z_1$ from the duct wall to the 'interface', show the progress of the phase change process in the axial direction. The approximate proportion of particles already melted or frozen at any cross section may be obtained from the knowledge of 'interface' location since this melted fraction is a function of the distance of the interface from the wall which is $\simeq \{\pi R_d^2 - \pi(R_d - z)^2\}/(\pi R_d^2) = (2 - z_1)z_1$, where $z_1 = z/R_d$.

*Constant wall temperature*

The most dominant parameters for the problem are the bulk 'Stefan number' and the concentration. Their effects are shown in Figs. 6 and 7. The Nusselt number can be considerably improved by reducing the bulk 'Stefan number', which corresponds to increasing the 'latent heat' of the slurry. The effect of increasing the concentration is twofold: it decreases the 'Stefan number' and raises the conductivity enhancement factor. Based on a perturbation solution for heat transfer from a flat plate to a phase change slurry, Chen and Chen [10] had showed that the local Nusselt number for low $Ste_b$ is proportional to $Ste_b^{-1/3} \times (1 - Ste_b/6 - \cdots)$. This is also found to be approximately true in this case for $Ste_b \leqslant 0.5$. The effects of the $Pe_f(R_p/R_d)^2$ product and the radius ratio are relatively weak. For example, at $x_1 = 0.01$, the change in the mean Nusselt number is less than 6% when $Pe_f(R_p/R_d)^2$ varies from 1 to 4, and less than 5% when the radius ratio varies from 50 to 200. The effect is greater at a lower $x_1$ and smaller at a higher $x_1$. For a radius ratio in the 200–400 range, the change in mean Nusselt number is negligibly small. It suggests that for very large radius ratios, the heat transfer in the slurry is controlled by diffusion in the flow field rather than diffusion in the particles. Therefore, we may conclude that variation of particle size due to the manufacturing process is not very critical to the thermal characteristics of phase change slurries. The effect of the conductivity ratio is essentially negligible in the range of the present study and may be completely dropped from the parameter group.

In general, the mean Nusselt number for the phase change slurry flow is about 1.5–2.5 times higher than

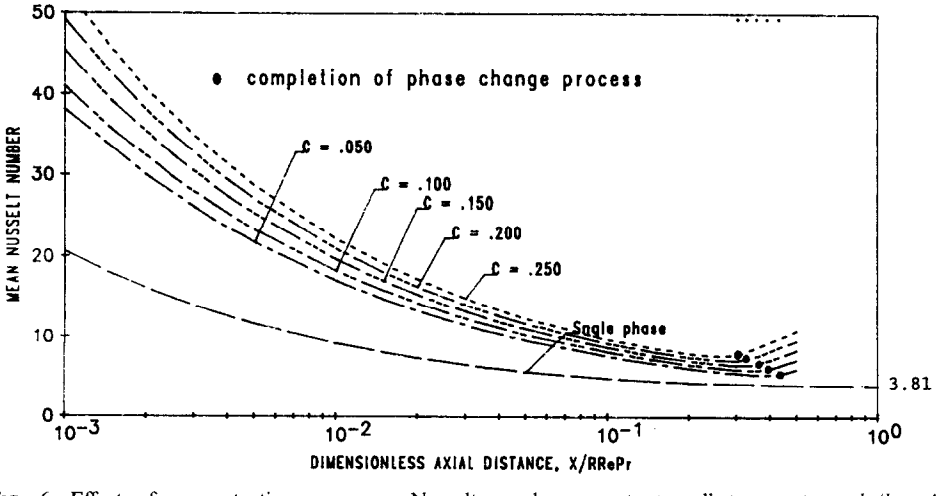


FIG. 6. Effect of concentration on mean Nusselt number: constant wall temperature. $k_p/k_f = 4$, $Pe_f(R_p/R_d)^2 = 1.0$, $R_d/R_p = 100$, $Ste_b = 0.5$.

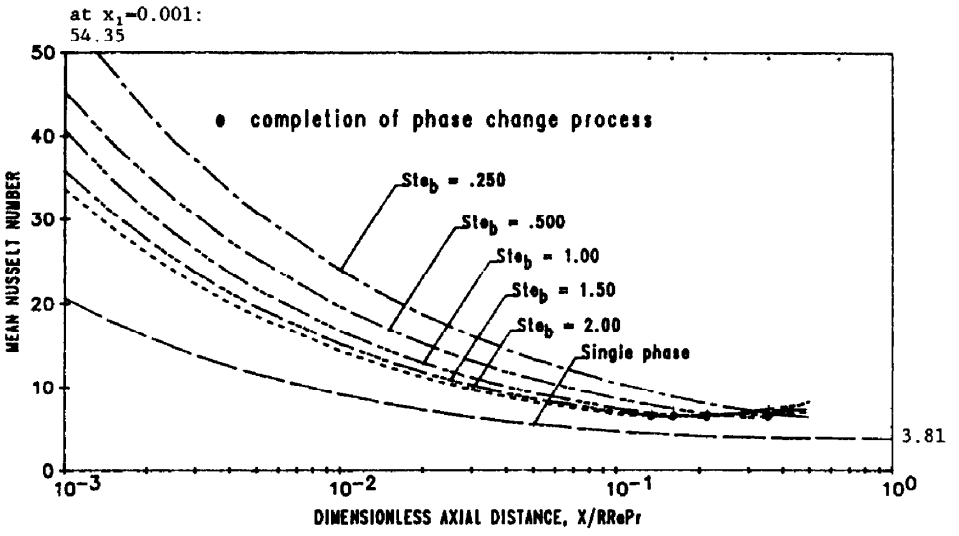


FIG. 7(a). Effect of Stefan number on mean Nusselt number: constant wall temperature. $c = 0.15$, $k_p/k_f = 4.0$, $Pe_f(R_p/R_d)^2 = 1.0$, $R_d/R_p = 100$.

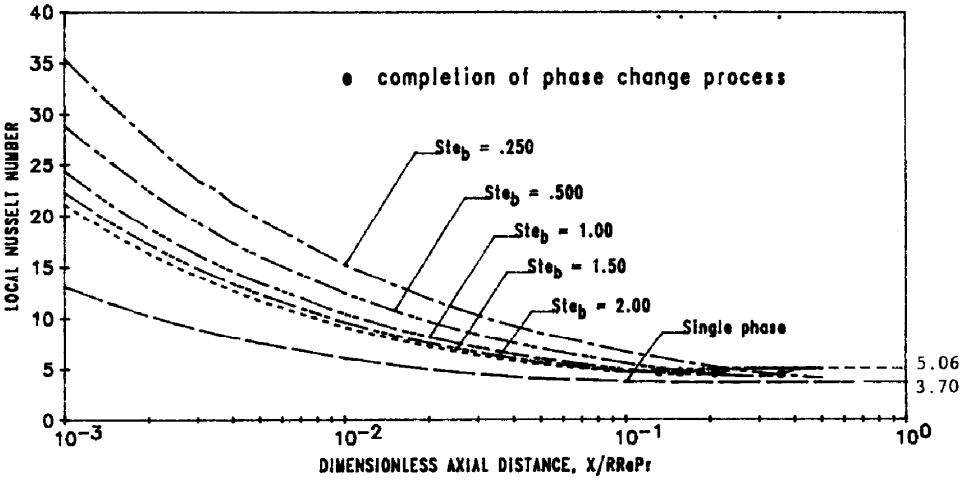


FIG. 7(b). Effect of Stefan number on local Nusselt number: constant wall temperature. $c = 0.15$, $k_p/k_f = 4.0$, $Pe_f(R_p/R_d)^2 = 1.0$, $R_d/R_p = 100$.

that of the pure fluid flow (Fig. 7). In addition, in the slurry system, the wall/fluid temperature difference is maintained substantially higher than the single phase flow as shown in Fig. 8. Therefore, a heat flux of about 2–4 times higher than that of the single phase flow may be achieved by the phase change slurry system. Sample calculations in the Appendix show the comparison in terms of dimensional quantities. Once all the particles are completely melted, the effect of enhanced thermal conductivity due to micro-convective effects tends to quickly lower the bulk mean temperature. This causes the mean Nusselt numbers to rise at the same period as can be seen at the ends of the curves in Fig. 7.

*Constant wall heat flux*

The effects of parameters discussed earlier in this section were found to be similar to the case of constant wall temperature. Figure 10 shows that the local Nusselt number is about 1.5–4 times higher than the single phase flow. Moreover, the bulk mean temperature rise is effectively suppressed to about half of the single phase flow. The combined effects can be utilized in the forms of flow reduction, or more effective control of the wall temperature as demonstrated by sample calculations in the Appendix.

It is interesting to note that the local Nusselt number decreases until all the particles become completely melted. After that it rises slightly and then remains

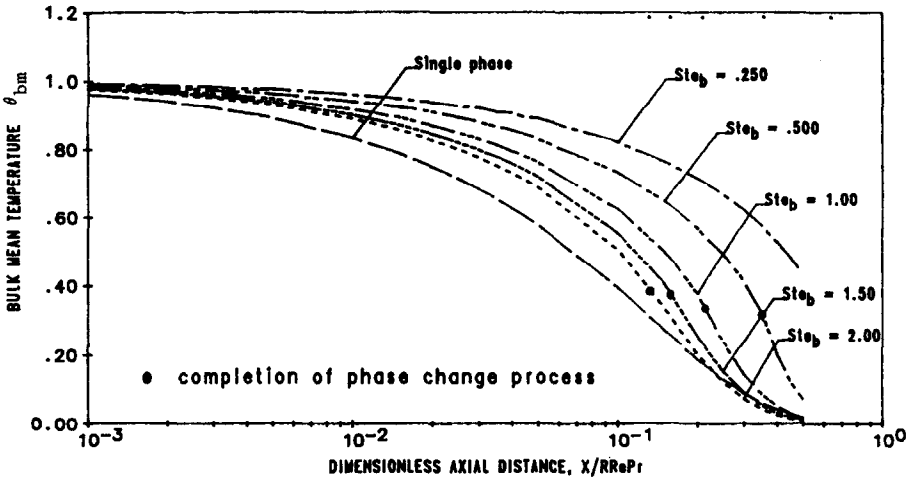


FIG. 8. Effect of Stefan number on bulk mean temperature: constant wall temperature. $c = 0.15$, $k_p/k_f = 4.0$, $Pe_f(R_p/R_d)^2 = 1.0$, $R_d/R_p = 100$.

constant. Such characteristics can be explained clearly from examination of the temperature profile development in Fig. 13 along with equation (33). During the period before the phase change completion, the profiles change such that the flat portion is shortened (see curve of $Ste_b = 1.00$, for example), therefore, $\theta_w - \theta_{bm}$ increases and $Nu_x$ decreases. After the completion, the profiles flatten, $\theta_w - \theta_{bm}$ decreases, and hence $Nu_x$ increases. The profiles finally become fully developed, and $\theta_w - \theta_{bm}$ and $Nu_x$ remain constant.

*Pressure drop in slurry flow*

In laminar duct flow of Newtonian fluid, the pressure drop is a linear function of fluid viscosity. For slurries which can be treated as Newtonian homogeneous fluids, the pressure drop may be calculated from the same relationship [18]. At higher concentrations, however, slurry flow characteristics may slightly deviate from the single phase flow [11]. Since the presence of particles in a fluid results in higher bulk viscosity than that of the suspending fluid, pressure loss in a slurry flow is greater than a single phase flow under the same flow condition. The viscosity of a slurry may be calculated from [32]

$$\frac{\mu_b}{\mu_f} = (1 - c - 1.16c^2)^{-2.5}. \tag{34}$$

In the concentration range of 0.10–0.20, the bulk viscosity is about 1.3–2.0 times higher than the suspending fluid. Therefore, the pressure drop is expected to be greater by the same proportion. This pressure loss penalty is however minor compared to the magnitude of the heat transfer enhancement shown in the Appendix.

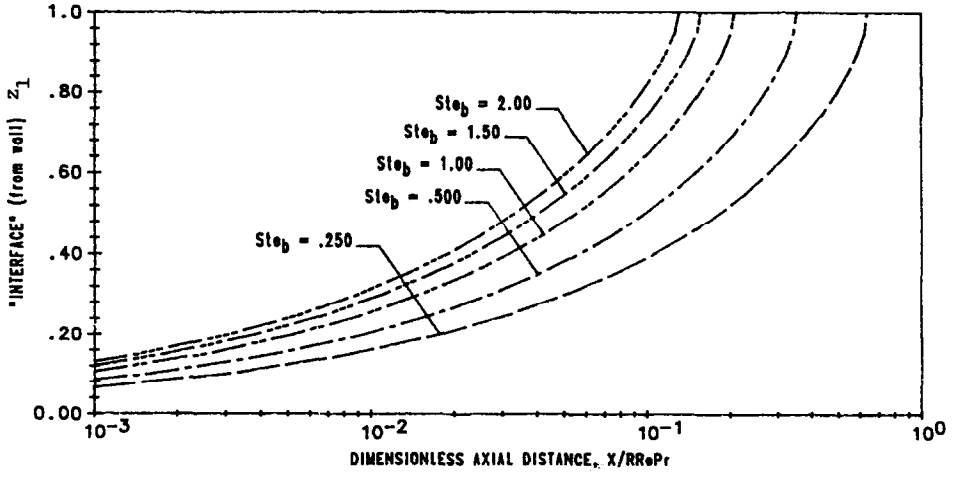


FIG. 9. Effect of Stefan number on interface location: constant wall temperature. $c = 0.15$, $k_p/k_f = 4.0$, $Pe_f(R_p/R_d)^2 = 1.0$, $R_d/R_p = 100$.

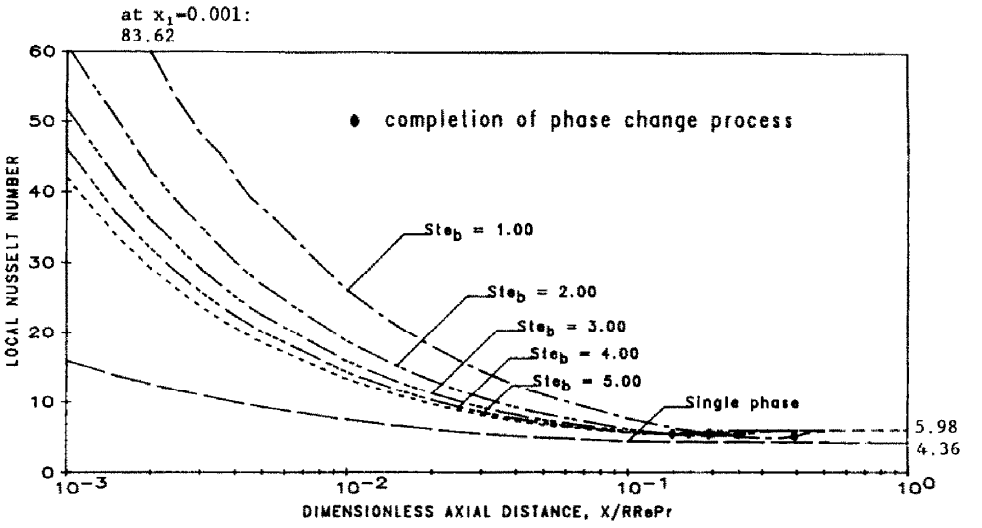


FIG. 10. Effect of Stefan number on local heat flux: constant wall heat flux. $c = 0.15$, $k_p/k_f = 4.0$, $Pe_f(R_p/R_d)^2 = 1.0$, $R_d/R_p = 100$.

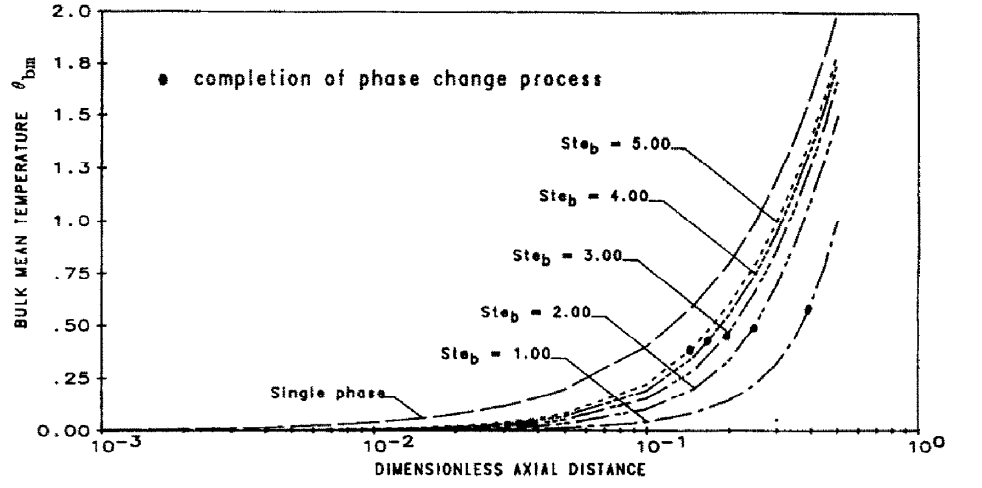


FIG. 11. Effect of Stefan number on bulk mean temperature: constant wall heat flux. $c = 0.15$, $k_p/k_f = 4.0$, $Pe_f(R_p/R_d)^2 = 1.0$, $R_d/R_p = 100$.

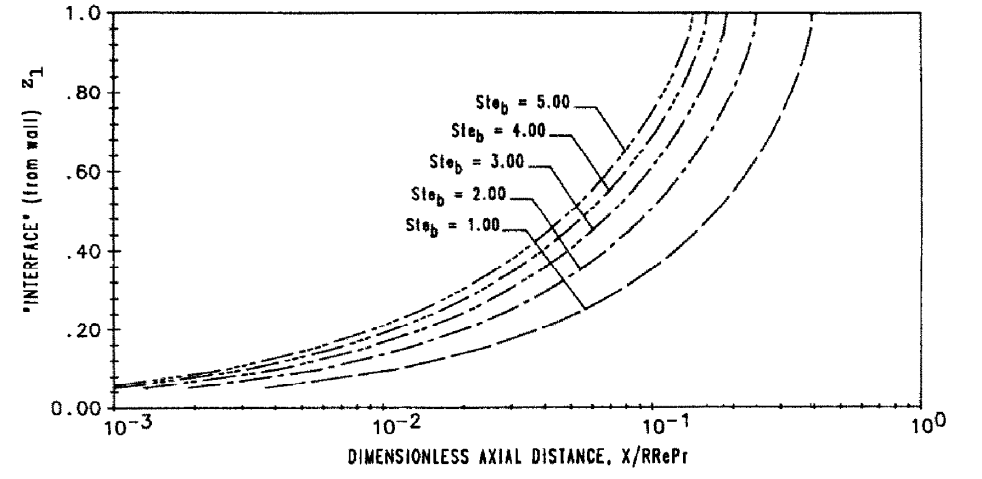


FIG. 12. Effect of Stefan number on interface location: constant wall heat flux. $c = 0.15$, $k_p/k_f = 4.0$, $Pe_f(R_p/R_d)^2 = 1.0$, $R_d/R_p = 100$.

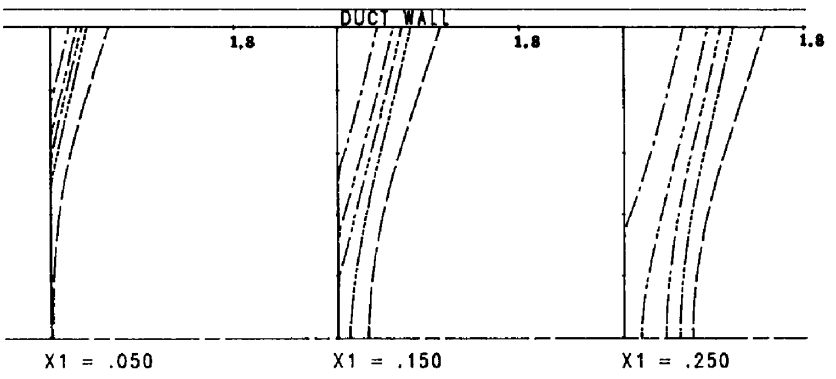


FIG. 13. Temperature profiles of phase change slurry flow compared to single phase flow at various axial locations along a duct: constant wall heat flux. $c = 0.15$, $k_p/k_f = 4.0$, $Pe_f(R_p/R_d)^2 = 1.0$, $R_d/R_p = 100$. ——, single phase flow; – – – –, $Ste_b = 1.0$; — — — —, $Ste_b = 2.0$; — — — — —, $Ste_b = 3.0$; — — — — — —, $Ste_b = 5.0$.

## SUMMARY

The governing equations for heat transfer of microencapsulated phase change material slurry flow in circular ducts have been formulated. Heat generation (or absorption) due to phase change in the particles was included in the energy equation as a heat source. The enhancement of thermal conductivity due to the particle/fluid interactions was also taken into consideration. The dimensionless parameters are the bulk 'Stefan number', the particle concentration, a modified Peclet number, the particle-to-tube radius ratio and the conductivity ratio.

The bulk 'Stefan number' and the concentration are the most dominant parameters. The effect of $Pr_f(R_p/R_d)^2$ is relatively weak. The effect of the radius ratio is also weak but noticeable in the range of 50–200 and negligible for the ratio in the range of 200–400. It suggests that the variation of the particle size due to manufacturing processes is not critical to the thermal performance of the phase change slurry system.

The results show that the slurry system can effectively enhance the heat transfer coefficient and sustain the fluid temperature. Such improvements may be utilized in the form of increased heat transfer rate, flow reduction, or more effective control of the wall temperature.

*Acknowledgement*—The authors thank the Engineering Computer Center, University of Miami, for the computer time and the Florida High Technology and Industry Council for grant support.

## REFERENCES

1. D. V. Hale, M. J. Hoover and M. J. O'Neil. *Phase-change materials Handbook*. NASA CR-61363 (1971).
2. R. Hart and F. Thornton, Microencapsulation of phase change materials, Final Report Contract No. 82-80, Department of Energy, Ohio (1982).
3. K. E. Kasza and M. M. Chen, Development of enhanced heat transfer/transport/storage slurries for thermal-system improvement, Argonne Nat. Lab., ANL-82-50 (1982).
4. W. A. McMahon, Jr., W. W. Harlowe, Jr. and D. J. Mangold, Feasibility study of utilizing phase change coolant for protective garment, Final Rept. Contract No. DAAK60-81-C-0098, U.S. Army Natick Research and Development Command, Massachusetts (1982).
5. D. P. Colvin and J. C. Mulligan, Spacecraft heat rejection methods: active and passive heat transfer for electronic systems—Phase I, Final Report AFWAL-TR-86-3074 (1986).
6. S. Sengupta, Microencapsulated phase change material slurries for thermal management of electronic packages, Final Report, The Florida High Technology and Industry Council (1989).
7. P. A. Bahrami, Fusible pellet transport and storage of heat, ASME Paper No. 82-HT-32 (1982).
8. M. Telkes, Phase change thermal storage materials with crust forming stabilizers, U.S. Patent 4 187 189 (1980).
9. K. Kasza and M. M. Chen, Improvement of the performance of solar energy or waste heat utilization systems by using phase-change slurry as an enhanced heat transfer storage fluid, *J. Solar Energy Engng* **108**, 229–236 (1985).
10. K. Chen and M. M. Chen, An analytical and experimental investigation of the convective heat transfer of phase-change slurry flows, *Proc. Int. Symp. Multiphase Flows (II)*, August 1987, pp. 496–501. Zejiang University Press, China (1987).
11. A. S. Ahuja, Augmentation of heat transport in laminar flow of polystyrene suspensions: Part 1, *J. Appl. Phys.* **46**(8), 3408–3416 (1975).
12. A. S. Ahuja, Augmentation of heat transport in laminar flow of polystyrene suspensions: Part 2, *J. Appl. Phys.* **46**(8), 3417–3425 (1975).
13. C. W. Sohn and M. M. Chen, Microconvective thermal conductivity in disperse two-phase mixture as observed in a laminar flow, *J. Heat Transfer* **103**, 47–51 (1981).
14. C. W. Sohn and M. M. Chen, Heat transfer enhancement in laminar slurry pipe flows with power law thermal conductivities, *J. Heat Transfer* **106**, 539–542 (1984).
15. S. H. Maron and S. M. Fok, Rheology of synthetic latex: V. Flow behavior of low-temperature GR-S latex, *J. Colloid Sci.* **10**, 482–493 (1955).
16. S. H. Maron and A. E. Levy-Pascal, Rheology of synthetic latex: VI. The flow behavior of neoprene latex, *J. Colloid Sci.* **10**, 494–503 (1955).
17. I. R. Rutgers, Relative viscosity of suspensions of rigid spheres in Newtonian liquids, *Rheol. Acta* **2**(4), 305–348 (1962).
18. T. C. Aude, N. T. Cowper, T. L. Thompson and E. J.

Wasp, Slurry piping systems: trends, design methods, guidelines, *Chem. Engng* 74–90 (28 June 1971).
19. R. Darby, Hydrodynamics of slurry and suspensions. In *Encyclopedia of Fluid Mechanics* (Edited by N. P. Cheremisinoff), Vol. 5. Gulf, Houston (1986).
20. G. Segre and A. Silberberg, Behavior of macroscopic rigid spheres in Poisseuille flow: Part 2. Experimental results and interpretation, *J. Fluid Mech.* **14,** 136–157 (1962).
21. A. Karnis, H. L. Goldsmith and S. G. Mason, The flow of suspensions through tubes, *Can. J. Chem. Engng* 181–193 (August 1966).
22. G. F. Eveson, The rheological properties of stable suspensions of very small spheres at low rates of shear, *J. Oil Colour Chem. Assoc.* **40,** 456–477 (1957).
23. V. Vand, Viscosity of solutions and suspensions, *J. Phys. Coll. Chem.* **52,** 300–321 (1948).
24. J. C. Maxwell, *A Treatise on Electricity and Magnetism* (3rd Edn), Vol. I, pp. 440–441. Dover, New York (1954).
25. L. G. Leal, On the effective conductivity of dilute suspension of spherical drops in the limit of low particle Peclet number, *Chem. Engng Commun.* **1,** 21–31 (1973).
26. A. Nir and A. Acrivos, The effective thermal conductivity of sheared suspensions, *J. Fluid Mech.* **78**(1), 33–48 (1976).
27. L. C. Tao, Generalized numerical solutions of freezing a saturated liquid in cylinders and spheres, *A.I.Ch.E. Jl* **13**(1), 165–169 (1967).
28. W. M. Kays and M. E. Crawford, *Convective Heat and Mass Transfer* (2nd Edn). McGraw-Hill, New York (1980).
29. G. D. Raithby and K. G. T. Holland, Natural convection. In *Handbook of Heat Transfer Fundamentals* (Edited by W. M. Rohsenow, J. P. Hartnett and E. N. Ganic), (2nd Edn). McGraw-Hill, New York (1985).
30. S. K. Roy and S. Sengupta, The melting process within spherical enclosures, *J. Heat Transfer* **109,** 460–462 (1987).
31. E. N. Sieder and G. E. Tate, Heat transfer and pressure drop of liquids in tubes, *Ind. Engng Chem.* **28,** 1429–1435 (1936).
32. V. Vand, Theory of viscosity of concentrated suspensions, *Nature* **155,** 364–365 (1945).
33. A. Abhat, Low temperature latent heat thermal energy storage: heat storage materials, *Solar Energy* **30**(4), 313–332 (1983).
34. R. K. Shah and A. L. London, Laminar flow forced convection in ducts. In Supplement 1 to *Advances in Heat Transfer*. Academic Press, New York (1978).

## APPENDIX: SAMPLE CALCULATIONS

The calculations described below demonstrate the application of the present results and compares the performance of the phase change slurry system (15% concentration of 500 $\mu$m microcapsules) with the single phase flow under specified conditions. The following materials are used in the calculations: fluid, Fluorinert FC-77, property values as given by 3M Corp.; phase change material, $Na_2HPO_4 \cdot 12H_2O$, property values taken from ref. [33].

*Constant wall temperature*

Given a tube with length $L = 0.5$ m and diameter $D = 5$ mm. It is used to remove heat at a rate of $q_w = 0.191$ W cm$^{-2}$. Calculate and compare flow rate required for the slurry flow and the single phase flow. Assume an inlet temperature and a wall temperature of 20 and 32.5°C, respectively.

*Constant wall heat flux*

Given a tube with length $L = 0.5$ m and diameter $D = 5$ mm. It is used to remove heat which is generated at the rate of $q_w = 0.214$ W cm$^{-2}$. Calculate and compare flow rate required to maintain the wall temperature not higher than 45°C using the slurry and a single phase fluid. Assume the fluid enters the heat transfer section at temperature $T_{in} = 25$°C.

*Solution*

The solution technique for a slurry flow is completely analogous to that used for similar problems with a single phase fluid. Only the case for constant wall temperature will be solved here.

*Phase change slurry flow (constant wall temperature)*

Before starting the actual calculations, evaluate the Stefan number, 0.4.

Steps of calculations:

(1) Guess mean velocity $u_m$.
(2) Calculate $Pe_f(R_p/R_d)^2$; and $Pe_b = u_m D/\alpha_b$ and $x_1 = 2L/(D\,Pe_b)$.
(3) Read $Nu_m$ and $T_{out}$ from graphs, Figs. 7 and 8, for example.
(4) Calculate $h_m = Nu_m k_b/D$
$\Delta T_{ln} = (\Delta T_{in} - \Delta T_{out})/\ln(\Delta T_{in}/\Delta T_{out})$.
(5) Calculate $q_c = h_m \Delta T_{ln}$.
(6) Compare $q_c$ with $q_w$, if $q_c = q_w$ then answer:
if $q_c > q_w$ then reduce velocity and go to 1
if $q_c < q_w$ then increase velocity and go to 1.

The calculation steps above yield the following results: velocity – 0.022 m s$^{-1}$, outlet temperature = 22.4°C.

The results of both the problems posed above are summarized in Table A1.

Table A1. Summary of the comparisons

| | Heat flow (W cm$^{-2}$) | Fluid flow rate (m s$^{-1}$) | $\Delta T$ (°C) |
|---|---|---|---|
| | (1) Constant wall temperature | | |
| Single phase | 0.191 | 0.19 | 2.2[a] |
| Slurry | 0.191 | 0.022 | 2.4 |
| Slurry | 0.449 | 0.19 | 1.6 |
| | (2) Constant wall heat flux | | |
| Single phase | 0.214 | 0.27 | 20[b] |
| Slurry | 0.214 | 0.026 | 20 |
| Slurry | 0.214 | 0.27 | 5.4 |

[a] Fluid temperature rise, $T_{f,out} - T_{f,in}$.
[b] $T_{w,out} - T_{f,in}$.

## CONVECTION THERMIQUE FORCEE DANS DES BOUES ENCAPSULEES ET A CHANGEMENT DE PHASE: ECOULEMENT DANS DES CONDUITS CIRCULAIRES

**Résumé**—On présente les caractéristiques d'un écoulement boueux de matériau à changement de phase et encapsulé. L'équation d'énergie est formulée en prenant en compte l'absorption de chaleur (ou la libération) due au changement de phase et l'accroissement de conductivité induit par le mouvement des particules. La source thermique ou la fonction source de chaleur dans l'équation de l'énergie est obtenue à partir des solutions de solidification ou de fusion dans une sphère. La corrélation pour la conductivité effective de la boue est basée sur des résultats analytiques et expérimentaux disponibles. Les paramètres actifs sont la concentration en particules, un nombre global de Stefan, le rapport des rayons conduit/particule, le rapport des conductivités particule/fluide et un nombre de Péclet modifié. Pour les applications à température basse, on trouve que les paramètres dominants sont le nombre global de Stefan et la concentration. Les solutions numériques montrent que les flux thermiques peuvent être 2 à 4 fois plus grands que dans un écoulement monophasique.

## WÄRMEÜBERGANG BEI ERZWUNGENER KONVEKTION IN EINEM GEMENGE AUS MIKROGEKAPSELTEM SCHMELZBAREM MATERIAL: STRÖMUNG IN KREISRUNDEN KANÄLEN

**Zusammenfassung**—In der vorliegenden Arbeit werden Ergebnisse für den Wärmeübergang in einem in kreisrunden Kanälen strömendem Gemenge aus mikrogekapseltem schmelzbarem Material vorgestellt. Die Energiegleichung wird formuliert, wobei sowohl die Absorption (oder Freigabe) von Wärme infolge des Phasenänderungsvorgangs als auch die Erhöhung der Wärmeleitfähigkeit infolge der Partikelbewegung berücksichtigt werden. Der funktionale Ansatz für die Wärmequellen oder die Wärmeerzeugung in der Energiegleichung ergibt sich aus Lösungen für Erstarrungs- oder Schmelzvorgänge in einer Kugel. Die Korrelationsgleichung für die effektive Wärmeleitfähigkeit im Gemenge wird aufgrund verfügbarer analytischer und experimenteller Ergebnisse ermittelt. Die wichtigsten Einflußgrößen sind die Partikelkonzentration, die Stefan-Zahl des Gemenges, das Radienverhältnis von Kanal und Partikeln, das Verhältnis der Wärmeleitfähigkeiten von Partikeln und Fluid sowie eine modifizierte Peclet-Zahl. Bei niedrigen Temperaturen dominieren die Einflüsse der Stefan-Zahl und der Konzentration. Die numerischen Ergebnisse zeigen, daß die Wärmeströme ungefähr zwei- bis viermal größer sind als bei einer einphasigen Strömung.

## ВЫНУЖДЕННОКОНВЕКТИВНЫЙ ТЕПЛОПЕРЕНОС В СУСПЕНЗИЯХ МИКРОКАПСУЛ, СОДЕРЖАЩИХ МАТЕРИАЛ С ФАЗОВЫМ ПЕРЕХОДОМ: ТЕЧЕНИЕ В КАНАЛАХ КРУГЛОГО СЕЧЕНИЯ

**Аннотация**—Приводятся характеристики теплопереноса при течении суспензий микрокапсул, содержащих материал с фазовым переходом, в каналах круглого сечения. Уравнение сохранения энергии формулируется с учетом как поглощения (выделения) тепла, обусловленного процессом фазового перехода, так и с учетом увеличения теплопроводности, вызванного движением частиц. Источник тепла или функция тепловыделения в уравнении сохранения энергии определяется из решений, описывающих замерзание или плавление в сфере. Обобщающее соотношение для эффективной теплопроводности суспензии получено на основе имеющихся аналитических и экспериментальных результатов. Найдено, что определяющми параметрами являются концентрация частиц, объемное число Стефана, отношение радиусов канала и частиц, отношение теплопроводности частиц и жидкости, а также модифицированное число Пекле. Обнаружено, что при низких температурах доминирующими параметрами являются объемное число Стефана и концентрация. Численные решения показывают, что в таких суспензионных системах могут быть достигнуты тепловые потоки, значения которых в 2–4 раза выше, чем при однофазном течении.